

000 SCHEDULING YOUR LLM REINFORCEMENT LEARN- 001 002 003 004 005 006 007 008 009 010 011 012 013 014 015 016 017 018 019 020 021 022 023 024 025 026 027 028 029 030 031 032 033 034 035 036 037 038 039 040 041 042 043 044 045 046 047 048 049 050 051 052 053 SCHEDULING YOUR LLM REINFORCEMENT LEARN- ING WITH REASONING TREES

Anonymous authors

Paper under double-blind review

ABSTRACT

Using Reinforcement Learning with Verifiable Rewards (RLVR) to optimize Large Language Models (LLMs) can be conceptualized as progressively editing a query’s ‘Reasoning Tree’. This process involves exploring nodes (tokens) and dynamically modifying the model’s policy at each node. When combined with data scheduling, this process yields further gains in data efficiency and accuracy. However, existing RLVR data scheduling methods typically rely on path-based metrics to rank queries, overlooking the reasoning tree structures of these queries. In this paper, we introduce a novel metric, namely **Reasoning Score** (r-score), which measures the query’s learning difficulty based on the structure of its reasoning tree. Based on the r-score, we propose the **Reasoning Tree Schedule** (Re-Schedule), a scheduling algorithm that constructs a curriculum progressing from structurally simple (high r-score) to complex (low r-score) queries. Experiments on six math-reasoning benchmarks show that Re-Schedule significantly improves average accuracy, achieving gains of up to 3.2%. These strong results validate our approach and demonstrate that a structural understanding of the reasoning tree provides a more powerful and principled foundation for RLVR data scheduling.

1 INTRODUCTION

Advancing the complex reasoning capabilities of Large Language Models (LLMs) remains a significant challenge, particularly in domains like mathematical problem-solving. Reinforcement Learning with Verifiable Reward (RLVR) (Gao et al., 2024; DeepSeek-AI et al., 2025), especially through policy optimization methods like GRPO (Shao et al., 2024), has emerged as a powerful paradigm to address this challenge. As shown in Figure 1 (a), in this framework, the space of potential solution paths for a query can be modeled as a specific ‘Reasoning Tree’ (Wang et al., 2025b; Yang et al., 2025), where each node represents an intermediate reasoning step and each path represents a potential solution trajectory. From this perspective, RLVR operates as a dynamic ‘node-editing’ process of the reasoning tree: by rewarding correct paths and penalizing incorrect ones, the model iteratively refines its decision policy at each tree node. This optimization process gradually prunes branches that lead to low-quality or incorrect solutions, thereby improving overall reasoning accuracy.

In this paradigm, data scheduling plays a critical role in model performance (Hu et al., 2025; Yu et al., 2025; Li et al., 2025). The concept of data scheduling originates from curriculum learning (Bengio et al., 2009), which posits that models learn more effectively when training examples (queries) are organized in a meaningful sequence. Existing data scheduling strategies typically pre-define a ‘difficulty’ metric for queries, and schedule them from easy to hard to improve data efficiency and final performance (Xi et al., 2024; Chen et al., 2025b;a; Dai et al., 2025) However, from a reasoning tree perspective, current difficulty measure strategies exhibits a critical limitation: current methods estimate difficulty primarily via final solution accuracy, overlooking richer query-level characteristics such as the structural complexity of the reasoning tree. Accuracy alone is insufficient — low accuracy does not necessarily indicate that a query is inherently hard, and high accuracy does not guarantee ease of optimization. This inconsistency can undermine the efficacy of accuracy-based scheduling approaches. We illustrate this issue with the following examples.

To illustrate, consider two representative queries, **q1** and **q2**, whose reasoning trees are shown in Figure 1(a). As depicted in Figure 1(b), LLMs may exhibit low initial accuracy on **q1**, due to the presence of many incorrect solution trajectories (reasoning paths). However, its simple tree structure

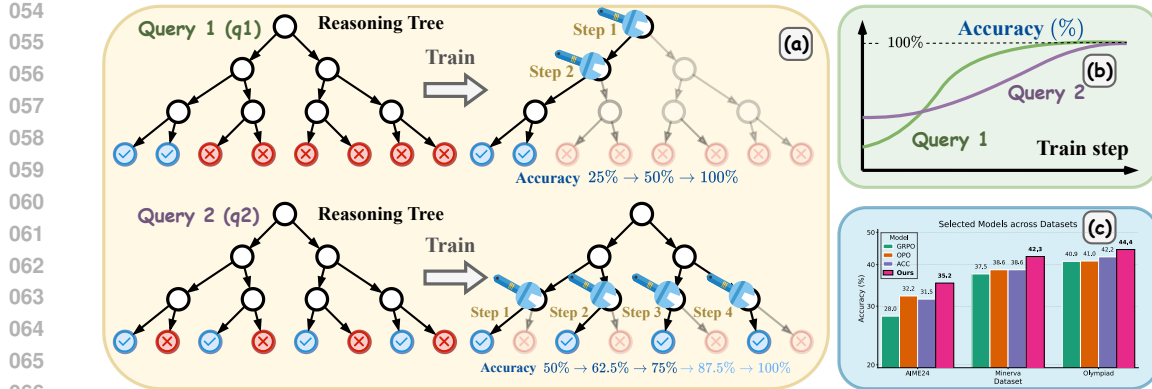


Figure 1: (a) A simple reasoning tree (q1) requires less node editing for performance improvement than a complex one (q2). (b) Consequently, q1 shows high training efficiency (steep learning curve) despite low initial accuracy, while q2’s complex structure leads to low efficiency. (c) Our method leverages this structural insight to significantly outperform baselines on various datasets.

means that modifying a few key decision nodes can yield substantial accuracy gains, indicating high learning efficiency despite the poor initial performance. In contrast, **q2** achieves higher initial accuracy, with roughly half of its trajectories being correct, yet these correct paths are scattered across disparate subtrees. This fragmented structure requires more extensive edits across numerous tree nodes, typically resulting in higher training difficulty and lower learning efficiency. Critically, existing path-based metrics will misinterpret **q1**’s low accuracy as high difficulty, thus assigning it a lower training weight, while incorrectly prioritizing the more difficult **q2**. Such path-based metrics may lead to a less efficient training process. This motivates our central research question: How can we move beyond path-based metrics to directly quantify a query’s true learning difficulty from its reasoning-tree structure?

To address this question, we introduce the **Reasoning Score** (r-score), a novel metric that quantifies a query’s learning potential based on its reasoning tree structure. We formalize this by framing the reinforcement learning training process as an optimization problem under a finite ‘node editing budget’, which we define as a fixed number of node editing operations. **Consequently, a query’s r-score is its maximum potential accuracy gain achievable within this limited editing budget.** This metric clearly explains the discrepancy in our example: **q1**, with its ‘concentrated’ error structure, yields a high r-score because a small budget (e.g., two edits) produces a massive accuracy gain (+75%). Conversely, **q2**’s ‘diffuse’ structure results in a low r-score, as the same budget only yields marginal improvement (+25%). Therefore, a higher r-score signifies a more tractable reasoning structure and greater learning efficiency, offering a more comprehensive assessment of difficulty than path-based metrics.

Building on the Reasoning Score, we propose the **Reasoning Tree Schedule (Re-Schedule)**, a novel data scheduling algorithm designed to guide RLVR training more efficiently. Our method consists of three main stages. First, an offline approximation of each query’s reasoning tree is constructed by sampling multiple solution trajectories from a base model. Second, this approximated reasoning tree is used to calculate each query’s reasoning score by simulating the editing process. Finally, we integrate the r-score as a dynamic weight into the RLVR loss function to form a schedule. This schedule prioritizes high-scoring (simple) queries in the initial training phases to accelerate convergence on simple queries. As training progresses, the weighting gradually shifts to lower-scoring (difficult) queries, enabling the model to master more challenging problems.

In summary, the main contributions of this paper are:

- We introduce the Reasoning Score (r-score), a new tree-based metric that measures a query’s learning efficiency rather than its path-based solution accuracy.
- We propose Re-Schedule, a data scheduling algorithm that uses the r-score to create an effective, easy-to-hard curriculum for RLVR.

108 • As shown in Figure 1(c), we empirically demonstrate that our approach significantly im-
 109 proves average accuracy, achieving gains of up to 3.2%, on complex reasoning tasks.
 110

111 **2 RELATED WORK**

113 **2.1 REINFORCEMENT LEARNING WITH VERIFIABLE REWARDS IN LLMs**

115 Reinforcement learning with verifiable reward (RLVR), where the reward is computed by a rule-
 116 based verification function, has been shown to be effective in improving the reasoning capabilities
 117 of LLMs (Gao et al., 2024; DeepSeek-AI et al., 2025; Kimi et al., 2025; Zeng et al., 2025; Wen
 118 et al., 2025; Song et al., 2025). Typically, RLVR frameworks assign a binary reward by comparing
 119 the model’s generated output against a ground-truth solution, indicating whether it is correct or in-
 120 correct. This reward design obviates the need for complex outcome-based or process-based reward
 121 models, offering a straightforward yet potent approach. Recent advancements in policy optimiza-
 122 tion algorithms, such as PPO and GRPO, have further refined this paradigm (Schulman et al., 2017;
 123 Kazemnejad et al., 2024; Yuan et al., 2025; Yue et al., 2025; Shao et al., 2024; Yu et al., 2025; Liu
 124 et al., 2025; Zhang et al., 2025; Hu, 2025). In contrast to these studies, which focus on algo-
 125 rithmic improvements, our work builds upon the standard GRPO framework with a primary focus on
 126 designing a more effective training data schedule.
 127

128 **2.2 DATA SCHEDULING ALGORITHM IN LLM REINFORCEMENT LEARNING**

129 Various data scheduling strategies have been proposed to enhance the reasoning capabilities in LLM
 130 Reinforcement Learning. These can be broadly categorized into static selection and dynamic ad-
 131 justment methods. Representative of static selection is LIMR (Li et al., 2025), which selected 1.4k
 132 examples from an 8.5k set for RLVR to match the performance of using the full set. In contrast,
 133 dynamic strategies make real-time adjustments during training. For instance, R^3 employs reverse
 134 curriculum reinforcement learning to simplify the model’s exploration space (Xi et al., 2024). **LPPO**
 135 (Chen et al., 2025b) utilize the gradient of accuracy to prioritize data, effectively treating learning
 136 difficulty as a derivative of performance. Similarly, **Seed-GRPO** (Chen et al., 2025a) employs se-
 137 mantic diversity (uncertainty) as a proxy for difficulty. Furthermore, **DELT** leverages training
 138 gradients to measure the quality and learnability of data (Dai et al., 2025), subsequently adjusting
 139 sample weights. However, these methods rely on outcome-based proxies (e.g., accuracy), effectively
 140 treating reasoning as a flat sequence. They overlook the inherent tree-structured solution space of
 141 reasoning tasks. In contrast, our approach explicitly leverages this topological structure. By ana-
 142 lyzing the Reasoning Tree, we directly quantify a query’s ‘structural learnability’, providing a more
 143 precise and principled measure of difficulty than performance statistics alone.
 144

145 **3 PRELIMINARIES**

146 **3.1 GROUP RELATIVE POLICY OPTIMIZATION**

147 The objective of the GRPO algorithm is to optimize a policy π_θ based on a group of generated
 148 responses (Shao et al., 2024; Yu et al., 2025). For a query q from a dataset \mathcal{D} , the policy generates
 149 G responses $\{o_i\}_{i=1}^G$. The token-level objective function is formulated as:

$$150 \mathcal{J}(\theta) = \mathbb{E}_{q \sim \mathcal{D}, \{o_i\}_{i=1}^G \sim \pi_{\text{old}}(\cdot | q)} \left[\frac{1}{\sum_{i=1}^G |o_i|} \sum_{i=1}^G \sum_{t=1}^{|o_i|} \min(r_{i,t} A_{i,t}, \text{clip}(r_{i,t}, 1 - \varepsilon, 1 + \varepsilon) A_{i,t}) \right], \quad (1)$$

151 where $r_{i,t} = \frac{\pi_\theta(o_{i,t} | q, o_{i,<t})}{\pi_{\text{old}}(o_{i,t} | q, o_{i,<t})}$ is the probability ratio of the token $o_{i,t}$ between the current and old
 152 policies. The advantage term $A_{i,t}$ is constant for all tokens within a single response and is calculated
 153 by normalizing the response’s reward R_i relative to the other responses in the group:

$$154 A_{i,t} = \frac{R_i - \text{mean}(\{R_k\}_{k=1}^G)}{\text{std}(\{R_k\}_{k=1}^G) + \delta}, \quad \forall t, \quad (2)$$

155 where δ is a small constant for numerical stability.
 156

162 Data scheduling algorithms can be formulated by introducing a weighting function $\omega(q, t)$ that mod-
 163 ules the contribution of each query $q \in \mathcal{D}$ and current epoch t to the overall objective. Specifically,
 164 the objective in Equation 1 is modified as follows:

$$\mathcal{J}_{\text{schedule}}(\theta) = \mathbb{E}_{q \sim \mathcal{D}, t} [\omega(q, t) \cdot (\text{original objective term for } q)]. \quad (3)$$

167 Note: In the equations above, we have abbreviated the full objective for clarity. For example, in an
 168 accuracy-based curriculum learning, the training weight ω is formulated as a function of the query’s
 169 accuracy $\text{ACC}(q)$ and current epoch t :

$$\alpha(\text{ACC}(q), t) = (1 - \gamma(t))\text{ACC}(q) + \gamma(t)(1 - \text{ACC}(q)), \quad (4)$$

$$\omega = \text{rank}(\alpha)\% \cdot \omega_{\max} + (1 - \text{rank}(\alpha)\%) \cdot \omega_{\min}. \quad (5)$$

170 Here, ω_{\max} and ω_{\min} are hyperparameters that define the maximum and minimum training weights
 171 (e.g., $\omega_{\max} = 0.8$, $\omega_{\min} = 0.2$); And $\text{rank}(\alpha)$ means calculating the reverse order of α in the entire
 172 dataset. The term $\gamma(t)$ is a scheduling function that progresses over time. Common choices for
 173 $\gamma(t)$ include a linear mapping, $\gamma(t) = t/T$, or a sigmoid function, $\gamma(t) = \sigma\left(\left(\frac{t}{T} - 0.5\right)\right)$, $\sigma(x) =$
 174 $(1 + e^{-x})^{-1}$, where T is the total number of epochs.

175 3.2 REASONING TREE

176 For complex reasoning tasks, the process of generating a solution can be conceptualized as traversing
 177 a ‘Reasoning Tree’. In this context, the root of the tree is the initial prompt, and each node represents
 178 a partial solution or an intermediate reasoning step. The branches extending from a node correspond
 179 to the possible next tokens or thought segments that the LLM can generate.

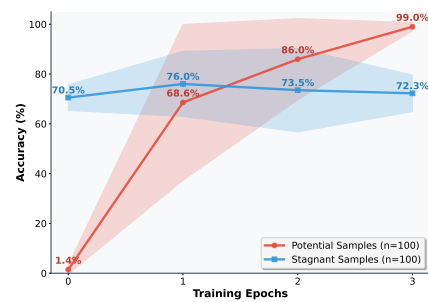
180 Due to the combinatorial explosion of possible solution paths, the complete reasoning tree is typ-
 181 ically computationally intractable. Therefore, analysis often relies on a structured approximation
 182 (e.g., a fixed-structure k-ary reasoning tree). Formally, an approximated reasoning tree is defined
 183 as a triplet $T = (\mathcal{N}, \mathcal{E}, \mathcal{R})$, where \mathcal{N} is the set of nodes, \mathcal{E} is the set of edges, and \mathcal{R} defines the
 184 parent-child relationships.

185 The components of the tree are described using the following notation: $\mathcal{N}_{\text{leaf}} \subset \mathcal{N}$ is the set of leaf
 186 nodes; For a given node $n_i \in \mathcal{N}$, $C(n_i)$ denotes the set of its immediate children and $\mathcal{L}(n_i)$ denotes
 187 the set of its leaf descendants. If n_i is a leaf node, then $\mathcal{L}(n_i) = \{n_i\}$. Within this framework, each
 188 non-leaf node $n_i \in \mathcal{N} \setminus \mathcal{N}_{\text{leaf}}$ represents a partial reasoning path, while a complete path to a leaf
 189 node $n_j \in \mathcal{N}_{\text{leaf}}$ corresponds to a full solution trajectory.

190 From this perspective, the RLVR optimization process is a dynamic ‘node editing’ of this reasoning
 191 tree. By rewarding correct paths and penalizing incorrect ones, the policy optimization algorithm
 192 adjusts the token probabilities at each node, effectively strengthening the branches that lead to cor-
 193 rect answers and weakening those that lead to errors. The structure of this tree—the distribution of
 194 correct and incorrect paths—is intrinsic to each problem sample and, as we will argue, is a key clue
 195 to its learning dynamics.

201 4 MOTIVATION

202 The premise of this work is that path-based metrics such
 203 as accuracy are poor indicators of a query’s true learn-
 204 ing difficulty. To illustrate our point, we supplement the
 205 example from the introduction with an experiment. As
 206 shown in Figure 2, we selected two distinct sets of 100
 207 queries each from the DAPA-Math-17K dataset, using
 208 the Qwen2.5-Math-7B model. The blue line represents
 209 ‘Stagnant Samples’—queries with high initial accuracy
 210 but complex reasoning structures (low r-score). Their
 211 flat learning curve indicates that despite high initial per-
 212 formance, they are difficult to improve further. In con-
 213 trast, the red line represents ‘Potential Samples’—queries
 214 with low initial accuracy but simple tree structures (high
 215 r-score). Their steep learning curve demonstrates high



216 Figure 2: Accuracy Progression During
 217 Training. The solid line represents the
 218 average accuracy, and the shaded area
 219 indicates the range.

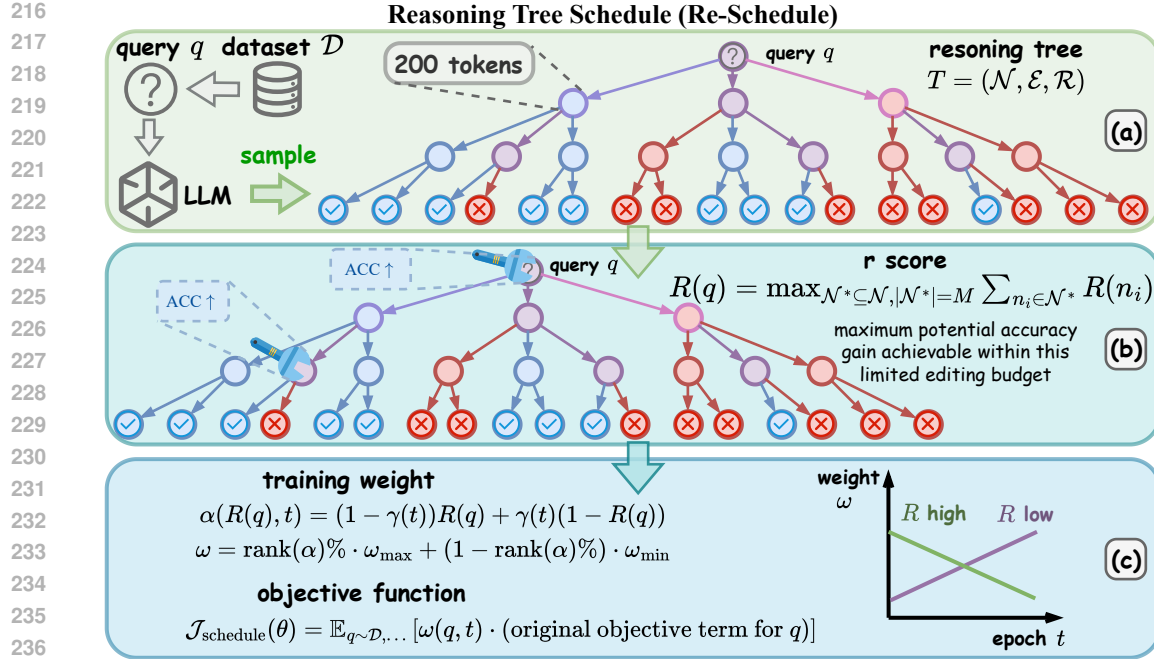


Figure 3: Overview of the **Reasoning Tree Schedule (Re-Schedule)** Algorithm. (a) **Tree Construction:** For each query, an approximate reasoning tree is constructed by sampling multiple solution paths from a base model (Note: This figure is for illustrative purposes only; our experiments use a tree with a depth of 4 and a width of 4, i.e., $k = 4, d = 4$). (b) **R-Score Calculation:** The tree’s structure is analyzed to compute the r-score, a metric quantifying the query’s learning potential. (c) **Dynamic Weighting:** The r-scores are used to dynamically weight each query during training, forming a curriculum that progresses from structurally simple (easy) to complex (hard) examples.

learnability, where a small amount of training yields significant gains. This discrepancy highlights that path-based metrics, like accuracy, are biased measurements for learning difficulty. This finding motivates us to design a new metric based on the structure of the reasoning tree.

5 METHOD

As illustrated in Figure 3, the **Reasoning Tree Schedule (Re-Schedule)** enhances reinforcement learning performance by creating a curriculum based on our novel metric, the **Reasoning Score (r-score)**. The r-score quantifies a query’s learning difficulty a priori based on the structure of its reasoning tree. Next, we will introduce the specific implementation details.

5.1 TREE CONSTRUCTION

As the entire reasoning tree is computationally intractable, we construct a manageable, fixed-structure k -ary approximation for each query q . The structure of this tree, \mathcal{T} , is defined by a branching factor k , a maximum depth d , and a token interval l (e.g., $k = 4, d = 4, l = 200$).

The construction process begins at the root node (the query q) and proceeds via a periodic branching strategy during response generation. Specifically, a branch is triggered immediately at the beginning of the response and subsequently at every l -token interval. As shown in Figure 3 (a), at each trigger, the current path splits into k independent sub-paths that continue to generate in parallel. This recursive branching process continues until a predefined maximum depth d is reached. To minimize computational overhead from this multi-path sampling, we use the Key-Value (KV) Cache, as all sibling branches share the same prefix.

In RLVR tasks, a solution’s quality is determined by the correctness of its final answer, which corresponds to a leaf node in our framework. Therefore, we define the quality of any intermediate

270 node n_i as the average accuracy of its leaf descendants, $\mathcal{L}(n_i)$. This is quantified using an accuracy
271 function:

$$272 \quad 273 \quad \text{ACC}(S) = \frac{\sum_{n_j \in S} \mathbb{I}(n_j \text{ is correct})}{|S|}, \quad 274 \quad (6)$$

275 where S is a set of leaf nodes and $\mathbb{I}(\cdot)$ is the indicator function. This allows us to assess quality
276 at different levels: the quality of a reasoning segment via $\text{ACC}(\mathcal{L}(n_i))$ and the model’s aggregate
277 performance on the query via $\text{ACC}(\mathcal{N}_{\text{leaf}})$.

279 5.2 R-SCORE CALCULATION

281 The r-score quantifies the learning potential of a node or query by measuring the maximum achievable
282 accuracy gain under a limited policy refining cost, like a limited node editing budget. Given this
283 idea, for any non-leaf node n_i , we define its r-score, $R(n_i)$, as the maximal accuracy gain achievable
284 by selecting its single best child branch and pruning all others. This is formulated as:

$$285 \quad 286 \quad R(n_i) = \max_{n_{\text{child}} \in \mathcal{C}(n_i)} \text{ACC}[\mathcal{N}_{\text{leaf}} \setminus \mathcal{L}(n_i) \cup \mathcal{L}(n_{\text{child}})] - \text{ACC}[\mathcal{N}_{\text{leaf}}]. \quad 287 \quad (7)$$

288 The overall r-score for a query, $R(q)$, estimates the total accuracy gain achievable under a budget
289 that limits modifications to a maximum of M nodes. It is the maximum sum of r-scores from any
290 set of M non-conflicting nodes (e.g., for a budget of $M = 4$):

$$291 \quad 292 \quad R(q) = \max_{\mathcal{N}^* \subseteq \mathcal{N}, |\mathcal{N}^*| = M} \sum_{n_i \in \mathcal{N}^*} R(n_i). \quad 293 \quad (8)$$

294 Two nodes are considered conflicting if one is located in a subtree that is implicitly pruned by the
295 optimal branch selection of the other.

296 Intuitively, solving Equation (7) represents the evaluation process of the sub-tree’s structure, while
297 a simpler structure of reasoning tree starting from n_i yields a higher $R(n_i)$. Combining the evalua-
298 tion $R(n_i)$ of each node n_i under a limited budget M , solving Equation (8) is to find the maximum
299 achievable accuracy gain over the reasoning tree, like exploring possible combinations of M nodes
300 and picking the best combination. Thus, a higher $R(q)$ indicates that substantial accuracy improve-
301 ments can be made by correcting just a few critical reasoning steps, signifying a structurally simple
302 and efficient-to-learn query.

304 5.3 DYNAMIC WEIGHTING

306 To strike a balance between data diversity and data scheduling, we propose a weighted scheduling
307 framework that dynamically adjusts data prioritization. Specifically, queries are assigned adaptive
308 weights determined by both training step t and r-score R . Specifically, when it is an early training
309 stage, higher weights are assigned to samples with higher r-scores (indicating lower learning dif-
310 ficulty), stabilizing the reinforcement learning. When RL training meets the later training phase,
311 queries’ weights will be redistributed gradually towards lower-r-score samples (higher learning dif-
312 ficulty) to enhance model generalization.

313 Motivated by this, the training weight ω of each query is formulated as

$$314 \quad 315 \quad \alpha(R(q), t) = (1 - \gamma(t))R(q) + \gamma(t)(1 - R(q)), \quad 316 \quad (9)$$

$$316 \quad 317 \quad \omega = \text{rank}(\alpha)\% \cdot \omega_{\text{max}} + (1 - \text{rank}(\alpha)\%) \cdot \omega_{\text{min}}, \quad (10)$$

318 where t is the current epoch; ω_{max} and ω_{min} are hyperparameters that define the maximum and min-
319 imum training weights; And $\text{rank}(\alpha)$ means calculating the reverse order of α in the entire dataset;
320 $\gamma(t)$ can be either linear mapping $\gamma(t) = \frac{t}{T}$ or sigmoid $\gamma(t) = \sigma\left(\left(\frac{t}{T} - 0.5\right)\right)$. The $\alpha(R(q), t)$ is
321 a monotonically varying function that down-weights high-scoring (simple) queries over time while
322 up-weighting lower-scoring (difficult) ones. This scheduling approach balances exploitation of eas-
323 ily learnable patterns and exploration of challenging instances, mitigating catastrophic forgetting of
underrepresented data distributions.

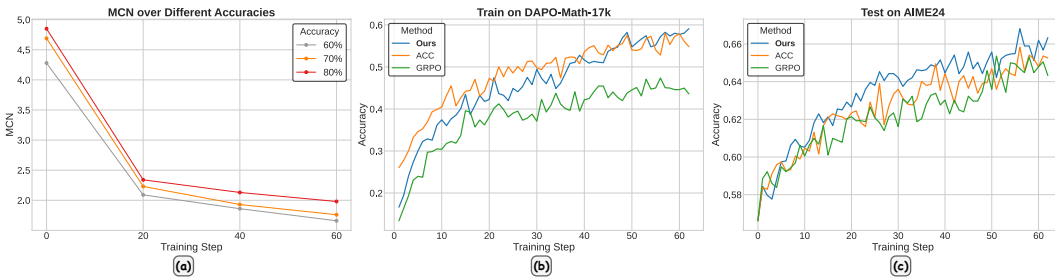


Figure 4: (a) The average MCN decreases over time, indicating successful tree optimization. (b) & (c) To compare metrics, we train models on the top 1/3 of data selected by each. The plots show the resulting (b) training accuracy and (c) test accuracy. The model used is Qwen2.5-Math-7B.

6 ANALYSIS

6.1 TRAINING AS REASONING TREE OPTIMIZATION

To empirically validate that the training process is optimizing reasoning trees, we conducted an experiment centered on a new metric: the Minimum Corrective Nodes (MCN). This metric is defined as the minimum number of node modifications required for the reasoning tree to achieve a specified target accuracy. A single node modification is counted as one token change; thus, a lower MCN signifies a well-structured reasoning tree. In our experiment, we tracked the MCN on the DAPA-Math-17K training set during the training of Qwen2.5-Math-7B, excluding queries where the base model’s accuracy was below 10%.

As shown in Figure 4(a), the average MCN across the training set exhibits a consistent downward trend as training progresses, regardless of the target accuracy. This result demonstrates that the reinforcement learning process effectively refines the model’s policy at critical decision nodes, thereby validating our central assumption that training is a process of reasoning tree optimization.

6.2 THE RELATIONSHIP BETWEEN R-SCORE AND LEARNING DIFFICULTY

In this experiment, we want to see which metric best identifies valuable queries for early-stage training. The process is as follows: First, we use each metric to select the top one-third of the data, creating several distinct subsets. Second, we train a separate model on each of these subsets for a single epoch. Finally, we evaluate the resulting models on both the training and test sets.

As shown in Figure 4(b), the subset selected by the ACC-based method initially shows higher average accuracy on the training set, as expected from its selection criteria. However, as training progresses, the model trained on the r-score-selected subset quickly surpasses it. This indicates that the r-score is more effective at identifying queries with low learning difficulty, rather than just initial accuracy.

The advantage of r-score is even more evident on the test set, as shown in Figure 4(c). Here, the model trained on the r-score-selected queries consistently outperforms both the ACC-based selection and a baseline with random query selection (GRPO). This confirms that the queries identified by the r-score provide the most effective learning signal, leading to better performance improvement and validating its capability in identifying the real difficulty of queries.

7 EXPERIMENT

7.1 RL TRAINING SETUPS

Training setting We conduct experiments on two different models, including Qwen2.5-Math-7B and Qwen2.5-7B. We adapt our training codebase from verl (Sheng et al., 2025) and follow the training recipe of standard GRPO. Our training data is DAPO-Math-17k (Yu et al., 2025), containing only math problems with integer ground-truth answers. Both the KL-divergence and entropy loss

378 terms are removed in our experiments. Generation batch size is set to 512. Training is performed
 379 with top-p value of 1.0 and temperature = 1.0.
 380

381 **Evaluation** We evaluated our models and baselines on six widely used mathematical reasoning
 382 benchmarks: AIME24, AIME25, AMC23 (Li et al., 2024), MATH-500 (Hendrycks et al., 2021),
 383 Minerva Math (Lewkowycz et al., 2022), and OlympiadBench (He et al., 2024). Validation is per-
 384 formed with a top-p value of 0.7 and temperature = 1.0 across all models and test sets. We use
 385 Math-Verify for training, validation, and final evaluation. **We report avg@32 for all datasets. All**
 386 **results are presented as percentages.**

387 **Baselines** For the throughout comparison, we compare our method against 7 baselines, including
 388 standard GRPO (Shao et al., 2024), SimpleRL-Zoo (Zeng et al., 2025), Eurus-PRIME(Cui et al.,
 389 2025), OPO (Hao et al., 2025), ACC (curriculum learning based on accuracy, using sigmoid weight-
 390 ing), LPPO (Chen et al., 2025b), and Seed-GRPO (Chen et al., 2025a).

391 **Our Methods** Re-Schedule is implemented with two weighting schemes: ‘linear’ and ‘sigmoid’.
 392 Unless otherwise specified, the reasoning trees in our experiments are constructed with a branching
 393 factor of $k = 4$, a maximum depth of $d = 4$, and a token interval of $l = 200$. The weighting
 394 schemes are defined as follows: 1. The ‘linear’ scheme uses $\gamma(t) = t/T$; 2. The ‘sigmoid’ scheme
 395 uses $\gamma(t) = \sigma\left(\left(\frac{t}{T} - 0.5\right)\right)$. For both, we set the total number of epochs $T = 10$. Details of the
 396 training setup can be found in the Appendix B.

397 7.2 MAIN EXPERIMENT

399 Table 1: Main benchmark results on **Qwen2.5-Math-7B**. All values are accuracies multiplied by
 400 100. Best results are in **bold**.

402 Model	AIME24	AIME25	AMC23	MATH500	Minerva	Olympiad	Avg.
403 Qwen2.5-Math-7B	13.8	5.3	44.6	39.6	9.9	13.8	21.2
Classical RLVR Methods							
405 GRPO	28.0	14.3	66.2	78.6	37.5	40.9	44.3
406 SimpleRL-Zoo	30.8	14.2	65.4	79.2	37.1	40.8	44.6
407 Eurus-PRIME	20.9	13.0	65.2	79.8	37.5	40.6	42.8
408 OPO	32.2	13.4	71.5	82.2	38.6	41.0	46.5
Scheduling Methods							
411 ACC _{sigmoid}	31.5	15.6	70.9	80.8	38.6	42.2	46.6
412 LPPO	32.8	14.9	63.3	79.2	39.0	40.6	45.0
413 Seed-GRPO	30.7	14.0	71.0	80.0	38.2	38.5	45.4
Our Methods							
415 Re-Schedule _{linear}	34.2	15.6	72.4	81.2	36.4	42.5	47.1
416 Re-Schedule _{sigmoid}	35.2	16.0	72.3	82.2	42.3	44.4	48.5

418 As shown in Tables 1 and 2, our Re-Schedule method consistently sets a new state-of-the-art, achiev-
 419 ing average scores of 48.5 on Qwen2.5-Math-7B and 44.5 on Qwen2.5-7B. It significantly outper-
 420 forms both scheduling baselines like ACC_{sigmoid} (by up to 3.2%) and classical RLVR methods like
 421 OPO/GRPO (by up to 3.8%). These results validate our central claim: that the reasoning tree’s
 422 structure, captured by our r-score, is a more effective way to measure the real learning difficulty of
 423 a query than path-based metrics like accuracy.

425 7.3 ABLATION EXPERIMENT

427 We investigate the impact of the reasoning tree’s structure by varying the branching factor k and
 428 maximum depth d . The choice of these parameters determines the fidelity of the approximated
 429 reasoning tree. While larger values for k and d theoretically provide a more accurate approximation
 430 and thus a more effective r-score, they also introduce a significant computational overhead. As
 431 shown in Table 3, our default configuration of $k = 4$ and $d = 4$ yields the best average performance
 (48.3%). **For more detailed analysis, please see Appendices C.3 and C.4.**

432 Table 2: Main benchmark results on **Qwen2.5-7B**. All values are accuracies multiplied by 100. Best
 433 results are in **bold**.

Model	AIME24	AIME25	AMC23	MATH500	Minerva	Olympiad	Avg.
Qwen2.5-7B	5.1	2.5	27.8	34.4	5.9	13.5	14.9
Classical RLVR Methods							
GRPO	15.6	8.8	62.5	78.2	38.6	40.4	40.7
SimpleRL-Zoo	17.0	9.6	64.7	76.6	31.6	40.3	40.0
OPO	16.6	8.4	64.6	74.6	31.6	40.3	39.4
Scheduling Methods							
ACC _{sigmoid}	16.7	9.8	68.6	79.0	34.2	39.4	41.3
LPPO	15.8	9.4	64.0	76.8	35.3	36.7	39.7
Seed-GRPO	13.3	6.0	63.3	76.6	32.4	36.3	38.0
Our Methods							
Re-Schedule _{linear}	18.4	12.2	68.6	80.4	41.2	42.1	43.8
Re-Schedule _{sigmoid}	18.2	14.0	69.2	81.0	41.5	43.3	44.5

451 Table 3: Ablation study on tree construction parameters. The default configuration (branching factor
 452 $k = 4$, depth $d = 4$) achieves the best performance.

Branch k	Depth d	AIME24	AIME25	AMC23	MATH500	Minerva	Olympiad	Avg.
4	4	34.2	16.0	71.1	81.8	42.3	44.4	48.3
3	5	33.8	14.8	68.4	79.6	42.3	42.8	46.9
5	3	31.7	14.2	70.4	81.0	41.9	43.0	47.0

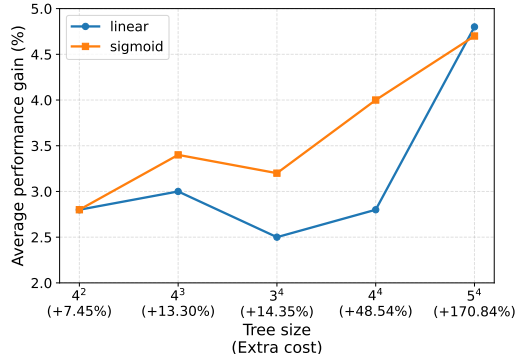
461 We analyze the sensitivity of our method to the minimum ω_{\min} and maximum ω_{\max} weight hyper-
 462 parameters, which control the dynamic range of the curriculum. Results in Table 4 show that our
 463 default setting of $\omega_{\min} = 0.5$ and $\omega_{\max} = 2.0$ achieves the highest average score (48.5). Decreasing
 464 the dynamic range by either reducing ω_{\max} (to 1.5) or increasing ω_{\min} (to 0.8) leads to performance
 465 degradation. This indicates that a sufficiently large weighting range is crucial for the curriculum to
 466 effectively differentiate between easy and hard samples. Conversely, an overly extreme range (e.g.,
 467 $\omega_{\min} = 0.2$) also degrades performance, possibly because the curriculum excessively under-weights
 468 difficult queries. By assigning them a minimal weight for a prolonged period, the model is prevented
 469 from learning difficult queries. Furthermore, for additional experiments on the design choices for
 470 the r-score calculation, please see Appendix C.1.

7.4 ANALYSIS EXPERIMENTS

7.4.1 COMPUTATIONAL COST ANALYSIS

477 As shown in Figure 5, we analyzed the trade-off
 478 between the offline tree construction cost and
 479 the resulting performance gain.

480 Table 5 presents the time cost measured on 8 ×
 481 H20 GPUs. While larger trees (4^4) incur higher
 482 preprocessing costs compared to smaller trees
 483 (3^3), the cost remains manageable relative to
 484 the total training time (approx. 46 hours for
 485 5 epochs), and the performance gains are sub-
 486 stantial.



487 Figure 5: Average performance gain versus reasoning tree size and computational cost.

486
487 Table 4: Ablation study on the weight function hyperparameters, ω_{\min} and ω_{\max} . The default setting
488 (0.5, 2.0) performs best.

ω_{\min}	ω_{\max}	AIME24	AIME25	AMC23	MATH500	Minerva	Olympiad	Avg.
0.5	2.0	35.2	16.0	72.3	82.2	42.3	44.4	48.5
0.5	1.5	31.4	15.4	72.3	81.8	38.1	42.5	46.9
0.5	3.0	33.5	15.0	69.1	81.8	37.5	41.0	46.3
0.8	2.0	36.6	13.6	71.1	81.6	37.1	43.8	47.3
0.2	2.0	33.5	13.9	71.0	80.0	38.2	41.6	46.4

497
498 Table 5: Computational cost vs. Performance gain. “Additional Cost” is relative to the total training
499 time.

Tree Size (k^d)	3³	4³	3⁴	4⁴ (Default)
Time Cost (hours)	3.48	6.21	6.70	22.67
Additional Cost	+7.45%	+13.30%	+14.35%	+48.54%
Avg Performance Gain	+3.2	+3.0	+3.2	+4.0

500 501 7.4.2 IMPACT OF ORDERING

502
503 Table 6: Comparison between Re-Schedule (Easy-to-Hard) and Reverse Schedule (Hard-to-Easy).

Schedule	AIME24	AIME25	AMC23	MATH500	Minerva	Olympiad	Avg
<i>Linear Mapping</i>							
Re-Schedule (Ours)	34.2	15.6	72.4	81.2	36.4	42.5	47.1
Reverse Schedule	31.9	14.0	67.6	81.0	37.8	41.8	45.7
<i>Sigmoid Mapping</i>							
Re-Schedule (Ours)	34.2	16.0	71.1	81.8	42.3	44.4	48.3
Reverse Schedule	30.2	15.4	67.1	80.6	34.9	40.2	44.7

519
520 To validate the “easy-to-hard” curriculum design, we compared our method against a “Reverse
521 Schedule” where lower r-score (harder) samples are prioritized first. As shown in Table 6, the Re-
522 verse Schedule leads to a significant drop in performance, confirming that starting with structurally
523 simple samples is crucial for effective learning.

524 8 CONCLUSIONS

525
526 In this work, we challenged the reliance on path-based metrics for RLVR data scheduling. We
527 introduced the r-score, a novel metric that quantifies learnability based on the structure of a query’s
528 reasoning tree, and proposed Re-Schedule, a curriculum learning algorithm built upon it. Extensive
529 experiments demonstrated that Re-Schedule consistently outperforms classical RLVR and existing
530 scheduling methods, validating that r-score is a more effective proxy for learnability than path-based
531 accuracy. Our findings establish that a structural understanding of the reasoning process provides a
532 more powerful and principled foundation for creating efficient training curricula in RLVR.

540
541 ETHICS STATEMENT542
543 We have manually reevaluated the dataset we created to ensure it is free of any potential for discrimination,
544 human rights violations, bias, exploitation, and any other ethical concerns.545
546 REPRODUCIBILITY STATEMENT547
548 To ensure the reproducibility of our findings, all source code and datasets used in our experiments
549 are included in the supplementary material. The provided materials are sufficient to replicate the
550 main results presented in this paper.551
552 REFERENCES553
554 Yoshua Bengio, Jérôme Louradour, Ronan Collobert, and Jason Weston. Curriculum learning. In
555 *Proceedings of the 26th annual international conference on machine learning*, pp. 41–48, 2009.556
557 Minghan Chen, Guikun Chen, Wenguan Wang, and Yi Yang. Seed-grpo: Semantic entropy enhanced
558 grp for uncertainty-aware policy optimization. *arXiv preprint arXiv:2505.12346*, 2025a.559
560 Xinjie Chen, Minpeng Liao, Guoxin Chen, Chengxi Li, Biao Fu, Kai Fan, and Xinggao Liu. From
561 data-centric to sample-centric: Enhancing llm reasoning via progressive optimization. *arXiv
562 preprint arXiv:2507.06573*, 2025b.563
564 Ganqu Cui, Lifan Yuan, Zefan Wang, Hanbin Wang, Wendi Li, Bingxiang He, Yuchen Fan, Tianyu
565 Yu, Qixin Xu, Weize Chen, Jiarui Yuan, Huayu Chen, Kaiyan Zhang, Xingtai Lv, Shuo Wang,
566 Yuan Yao, Xu Han, Hao Peng, Yu Cheng, Zhiyuan Liu, Maosong Sun, Bowen Zhou, and Ning
567 Ding. Process reinforcement through implicit rewards. *CoRR*, abs/2502.01456, 2025. doi: 10.
568 48550/ARXIV.2502.01456. URL <https://doi.org/10.48550/arXiv.2502.01456>.569
570 Yalun Dai, Yangyu Huang, Xin Zhang, Wenshan Wu, Chong Li, Wenhui Lu, Shijie Cao, Li Dong,
571 and Scarlett Li. Data efficacy for language model training. *arXiv preprint arXiv:2506.21545*,
572 2025.573
574 DeepSeek-AI, Daya Guo, Dejian Yang, Haowei Zhang, Junxiao Song, Ruoyu Zhang, Runxin Xu,
575 Qihao Zhu, Shirong Ma, Peiyi Wang, and et al Xiao Bi. Deepseek-r1: Incentivizing reasoning
576 capability in llms via reinforcement learning. *CoRR*, abs/2501.12948, 2025. doi: 10.48550/
577 ARXIV.2501.12948. URL <https://doi.org/10.48550/arXiv.2501.12948>.578
579 Jiaxuan Gao, Shusheng Xu, Wenjie Ye, Weilin Liu, Chuyi He, Wei Fu, Zhiyu Mei, Guangju Wang,
580 and Yi Wu. On designing effective RL reward at training time for LLM reasoning. *CoRR*,
581 abs/2410.15115, 2024. doi: 10.48550/ARXIV.2410.15115. URL <https://doi.org/10.48550/arXiv.2410.15115>.582
583 Yaru Hao, Li Dong, Xun Wu, Shaohan Huang, Zewen Chi, and Furu Wei. On-policy rl with optimal
584 reward baseline. *arXiv preprint arXiv:2505.23585*, 2025.585
586 Chaoqun He, Renjie Luo, Yuzhuo Bai, Shengding Hu, Zhen Leng Thai, Junhao Shen, Jinyi
587 Hu, Xu Han, Yujie Huang, Yuxiang Zhang, Jie Liu, Lei Qi, Zhiyuan Liu, and Maosong Sun.
588 Olympiadbench: A challenging benchmark for promoting AGI with olympiad-level bilingual
589 multimodal scientific problems. In Lun-Wei Ku, Andre Martins, and Vivek Srikumar (eds.), *Pro-
590 ceedings of the 62nd Annual Meeting of the Association for Computational Linguistics (Volume
591 1: Long Papers)*, ACL 2024, Bangkok, Thailand, August 11-16, 2024, pp. 3828–3850. Asso-
592 ciation for Computational Linguistics, 2024. doi: 10.18653/V1/2024.ACL-LONG.211. URL
593 <https://doi.org/10.18653/v1/2024.acl-long.211>.594
595 Dan Hendrycks, Collin Burns, Saurav Kadavath, Akul Arora, Steven Basart, Eric Tang,
596 Dawn Song, and Jacob Steinhardt. Measuring mathematical problem solving with
597 the MATH dataset. In Joaquin Vanschoren and Sai-Kit Yeung (eds.), *Proceedings
598 of the Neural Information Processing Systems Track on Datasets and Benchmarks
599 1, NeurIPS Datasets and Benchmarks 2021, December 2021, virtual*, 2021. URL
600 [https://datasets-benchmarks-proceedings.neurips.cc/paper/2021/
601 hash/be83ab3ecd0db773eb2dc1b0a17836a1-Abstract-round2.html](https://datasets-benchmarks-proceedings.neurips.cc/paper/2021/hash/be83ab3ecd0db773eb2dc1b0a17836a1-Abstract-round2.html).

594 Jian Hu. REINFORCE++: A simple and efficient approach for aligning large language models.
 595 *CoRR*, abs/2501.03262, 2025. doi: 10.48550/ARXIV.2501.03262. URL <https://doi.org/10.48550/arXiv.2501.03262>.

597

598 Jingcheng Hu, Yinmin Zhang, Qi Han, Dixin Jiang, Xiangyu Zhang, and Heung-Yeung Shum.
 599 Open-reasoner-zero: An open source approach to scaling up reinforcement learning on the base
 600 model, 2025. URL <https://arxiv.org/abs/2503.24290>.

601

602 Naman Jain, King Han, Alex Gu, Wen-Ding Li, Fanjia Yan, Tianjun Zhang, Sida Wang, Armando
 603 Solar-Lezama, Koushik Sen, and Ion Stoica. Livecodebench: Holistic and contamination free
 604 evaluation of large language models for code. *arXiv preprint arXiv:2403.07974*, 2024.

605

606 Amirhossein Kazemnejad, Milad Aghajohari, Eva Portelance, Alessandro Sordoni, Siva Reddy,
 607 Aaron C. Courville, and Nicolas Le Roux. Vineppo: Unlocking RL potential for LLM reasoning
 608 through refined credit assignment. *CoRR*, abs/2410.01679, 2024. doi: 10.48550/ARXIV.2410.
 609 01679. URL <https://doi.org/10.48550/arXiv.2410.01679>.

610

611 Kimi, Angang Du, Bofei Gao, Bowei Xing, Changjiu Jiang, Cheng Chen, Cheng Li, Chenjun Xiao,
 612 Chenzhuang Du, Chonghua Liao, Chunling Tang, Congcong Wang, Dehao Zhang, Enming Yuan,
 613 Enzhe Lu, Fengxiang Tang, Flood Sung, Guangda Wei, Guokun Lai, Haiqing Guo, Han Zhu,
 614 Hao Ding, Hao Hu, Hao Yang, Hao Zhang, Haotian Yao, Haotian Zhao, Haoyu Lu, Haoze Li,
 615 Haozhen Yu, Hongcheng Gao, Huabin Zheng, Huan Yuan, Jia Chen, Jianhang Guo, Jianlin Su,
 616 Jianzhou Wang, Jie Zhao, Jin Zhang, Jingyuan Liu, Junjie Yan, Junyan Wu, Lidong Shi, Ling Ye,
 617 Longhui Yu, Mengnan Dong, Neo Zhang, Ningchen Ma, Qiwei Pan, Qucheng Gong, Shaowei
 618 Liu, Shengling Ma, Shupeng Wei, Sihan Cao, Siying Huang, Tao Jiang, Weihao Gao, Weimin
 619 Xiong, Weiran He, Weixiao Huang, Wenhai Wu, Wenyang He, Xianghui Wei, Xianqing Jia,
 620 Xingzhe Wu, Xinran Xu, Xinxing Zu, Xinyu Zhou, Xuehai Pan, Y. Charles, Yang Li, Yangyang
 621 Hu, Yangyang Liu, Yanru Chen, Yeqie Wang, Yibo Liu, Yidao Qin, Yifeng Liu, Ying Yang, Yiping
 622 Bao, Yulun Du, Yuxin Wu, Yuzhi Wang, Zaida Zhou, Zhaoji Wang, Zhaowei Li, Zhen Zhu, Zheng
 623 Zhang, Zhexu Wang, Zhilin Yang, Zhiqi Huang, Zihao Huang, Ziyao Xu, and Zonghan Yang.
 624 Kimi k1.5: Scaling reinforcement learning with llms. *CoRR*, abs/2501.12599, 2025. doi: 10.
 625 48550/ARXIV.2501.12599. URL <https://doi.org/10.48550/arXiv.2501.12599>.

626

627 Aitor Lewkowycz, Anders Andreassen, David Dohan, Ethan Dyer, Henryk Michalewski, Vinay V.
 628 Ramasesh, Ambrose Sloane, Cem Anil, Imanol Schlag, Theo Gutman-Solo, Yuhuai Wu, Behnam
 629 Neyshabur, Guy Gur-Ari, and Vedant Misra. Solving quantitative reasoning problems with lan-
 630 guage models. In Sanmi Koyejo, S. Mohamed, A. Agarwal, Danielle Belgrave, K. Cho, and A. Oh
 631 (eds.), *Advances in Neural Information Processing Systems 35: Annual Conference on Neural In-
 632 formation Processing Systems 2022, NeurIPS 2022, New Orleans, LA, USA, November 28 - De-
 633 cember 9, 2022*, 2022. URL http://papers.nips.cc/paper_files/paper/2022/hash/18abbeef8cfe9203fdf9053c9c4fe191-Abstract-Conference.html.

634

635 Jia Li, Edward Beeching, Lewis Tunstall, Ben Lipkin, Roman Soletskyi, Shengyi Huang, Kashif
 636 Rasul, Longhui Yu, Albert Q Jiang, Ziju Shen, et al. Numinamath: The largest public
 637 dataset in ai4maths with 860k pairs of competition math problems and solutions. *Hugging
 638 Face repository*, 13:9, 2024. URL http://faculty.bicmr.pku.edu.cn/~dongbin/Publications/numina_dataset.pdf.

639

640 Xuefeng Li, Haoyang Zou, and Pengfei Liu. LIMR: less is more for RL scaling. *CoRR*,
 641 abs/2502.11886, 2025. doi: 10.48550/ARXIV.2502.11886. URL <https://doi.org/10.48550/arXiv.2502.11886>.

642

643 Zichen Liu, Changyu Chen, Wenjun Li, Penghui Qi, Tianyu Pang, Chao Du, Wee Sun Lee, and Min
 644 Lin. Understanding r1-zero-like training: A critical perspective. *CoRR*, abs/2503.20783, 2025.
 645 doi: 10.48550/ARXIV.2503.20783. URL <https://doi.org/10.48550/arXiv.2503.20783>.

646

647 John Schulman, Filip Wolski, Prafulla Dhariwal, Alec Radford, and Oleg Klimov. Proximal policy
 648 optimization algorithms. *CoRR*, abs/1707.06347, 2017. URL <http://arxiv.org/abs/1707.06347>.

648 Zhihong Shao, Peiyi Wang, Qihao Zhu, Runxin Xu, Junxiao Song, Mingchuan Zhang, Y. K. Li,
 649 Y. Wu, and Daya Guo. Deepseekmath: Pushing the limits of mathematical reasoning in open
 650 language models. *CoRR*, abs/2402.03300, 2024. doi: 10.48550/ARXIV.2402.03300. URL
 651 <https://doi.org/10.48550/arXiv.2402.03300>.

652

653 Guangming Sheng, Chi Zhang, Zilingfeng Ye, Xibin Wu, Wang Zhang, Ru Zhang, Yanghua Peng,
 654 Haibin Lin, and Chuan Wu. Hybridflow: A flexible and efficient rlhf framework. In *Proceedings
 655 of the Twentieth European Conference on Computer Systems*, pp. 1279–1297, 2025.

656

657 Mingyang Song, Mao Zheng, Zheng Li, Wenjie Yang, Xuan Luo, Yue Pan, and Feng Zhang.
 658 Fastcurl: Curriculum reinforcement learning with progressive context extension for efficient train-
 659 ing r1-like reasoning models. *CoRR*, abs/2503.17287, 2025. doi: 10.48550/ARXIV.2503.17287.
 660 URL <https://doi.org/10.48550/arXiv.2503.17287>.

661

662 Jiakang Wang, Runze Liu, Fuzheng Zhang, Xiu Li, and Guorui Zhou. Stabilizing knowledge, pro-
 663 moting reasoning: Dual-token constraints for rlvr. *arXiv preprint arXiv:2507.15778*, 2025a.

664

665 Shenzhi Wang, Le Yu, Chang Gao, Chujie Zheng, Shixuan Liu, Rui Lu, Kai Dang, Xionghui Chen,
 666 Jianxin Yang, Zhenru Zhang, et al. Beyond the 80/20 rule: High-entropy minority tokens drive
 667 effective reinforcement learning for llm reasoning. *arXiv preprint arXiv:2506.01939*, 2025b.

668

669 Liang Wen, Yunke Cai, Fenrui Xiao, Xin He, Qi An, Zhenyu Duan, Yimin Du, Junchen Liu, Lifu
 670 Tang, Xiaowei Lv, Haosheng Zou, Yongchao Deng, Shousheng Jia, and Xiangzheng Zhang.
 671 Light-r1: Curriculum sft, DPO and RL for long COT from scratch and beyond. *CoRR*,
 672 abs/2503.10460, 2025. doi: 10.48550/ARXIV.2503.10460. URL <https://doi.org/10.48550/arXiv.2503.10460>.

673

674 Zhiheng Xi, Wenxiang Chen, Boyang Hong, Senjie Jin, Rui Zheng, Wei He, Yiwen Ding, Shichun
 675 Liu, Xin Guo, Junzhe Wang, Honglin Guo, Wei Shen, Xiaoran Fan, Yuhao Zhou, Shihan Dou,
 676 Xiao Wang, Xinbo Zhang, Peng Sun, Tao Gui, Qi Zhang, and Xuanjing Huang. Training large
 677 language models for reasoning through reverse curriculum reinforcement learning. In *Forty-first
 678 International Conference on Machine Learning, ICML 2024, Vienna, Austria, July 21-27, 2024*.
 679 OpenReview.net, 2024. URL <https://openreview.net/forum?id=t82Y3fmRtk>.

680

681 Zhicheng Yang, Zhijiang Guo, Yinya Huang, Xiaodan Liang, Yiwei Wang, and Jing Tang. Treerpo:
 682 Tree relative policy optimization. *arXiv preprint arXiv:2506.05183*, 2025.

683

684 Qiying Yu, Zheng Zhang, Ruofei Zhu, Yufeng Yuan, Xiaochen Zuo, Yu Yue, Tiantian Fan, Gaohong
 685 Liu, Lingjun Liu, Xin Liu, Haibin Lin, Zhiqi Lin, Bole Ma, Guangming Sheng, Yuxuan Tong, Chi
 686 Zhang, Mofan Zhang, Wang Zhang, Hang Zhu, Jinhua Zhu, Jiaze Chen, Jiangjie Chen, Chengyi
 687 Wang, Hongli Yu, Weinan Dai, Yuxuan Song, Xiangpeng Wei, Hao Zhou, Jingjing Liu, Wei-Ying
 688 Ma, Ya-Qin Zhang, Lin Yan, Mu Qiao, Yonghui Wu, and Mingxuan Wang. DAPO: an open-
 689 source LLM reinforcement learning system at scale. *CoRR*, abs/2503.14476, 2025. doi: 10.
 690 48550/ARXIV.2503.14476. URL <https://doi.org/10.48550/arXiv.2503.14476>.

691

692 Yufeng Yuan, Yu Yue, Ruofei Zhu, Tiantian Fan, and Lin Yan. What's behind ppo's collapse in
 693 long-cot? value optimization holds the secret. *CoRR*, abs/2503.01491, 2025. doi: 10.48550/
 694 ARXIV.2503.01491. URL <https://doi.org/10.48550/arXiv.2503.01491>.

695

696 Yu Yue, Yufeng Yuan, Qiying Yu, Xiaochen Zuo, Ruofei Zhu, Wenyuan Xu, Jiaze Chen, Chengyi
 697 Wang, TianTian Fan, Zhengyin Du, Xiangpeng Wei, Xiangyu Yu, Gaohong Liu, Juncai Liu,
 698 Lingjun Liu, Haibin Lin, Zhiqi Lin, Bole Ma, Chi Zhang, Mofan Zhang, Wang Zhang, Hang
 699 Zhu, Ru Zhang, Xin Liu, Mingxuan Wang, Yonghui Wu, and Lin Yan. Vapo: Efficient and
 700 reliable reinforcement learning for advanced reasoning tasks, 2025. URL <https://arxiv.org/abs/2504.05118>.

701

702 Weihao Zeng, Yuzhen Huang, Qian Liu, Wei Liu, Keqing He, Zejun Ma, and Junxian He. Simplerl-
 703 zoo: Investigating and taming zero reinforcement learning for open base models in the wild.
 704 *CoRR*, abs/2503.18892, 2025. doi: 10.48550/ARXIV.2503.18892. URL <https://doi.org/10.48550/arXiv.2503.18892>.

702 Xiaojiang Zhang, Jinghui Wang, Zifei Cheng, Wenhao Zhuang, Zheng Lin, Minglei Zhang, Shaojie
703 Wang, Yinghan Cui, Chao Wang, Junyi Peng, et al. Srpo: A cross-domain implementation of
704 large-scale reinforcement learning on llm. *arXiv preprint arXiv:2504.14286*, 2025. URL <https://arxiv.org/abs/2504.14286>.
705
706
707
708
709
710
711
712
713
714
715
716
717
718
719
720
721
722
723
724
725
726
727
728
729
730
731
732
733
734
735
736
737
738
739
740
741
742
743
744
745
746
747
748
749
750
751
752
753
754
755

756 **A USAGE OF LLMs**
757758 Throughout the preparation of this manuscript, Large Language Models (LLMs) were utilized as a
759 writing and editing tool. Specifically, we employed LLMs to improve the clarity and readability of
760 the text, refine sentence structures, and correct grammatical errors. All final content, including the
761 core scientific claims, experimental design, and conclusions, was conceived and written by us, and
762 we take full responsibility for the final version of this paper.
763764 **B DETAILS OF EXPERIMENTAL SETUP**
765766 All algorithms are implemented based on the official GRPO codebase within the VeRL framework.
767 We use a learning rate of 1e-6 without warm-up across all experiments. At each rollout step, we
768 generate 8 answers for each of 512 sampled questions, then split the data into 16 mini-batches and
769 train the policy network for 16 gradient steps. Models are trained for at most 150 rollout steps.
770 Unless otherwise specified, we follow GRPO’s default design choices with token-level loss normal-
771 ization without dynamic sampling and KL regularization. For all models, the maximum input length
772 is 1024 and the minimum input length is 3072. All the experiments were conducted on H20 GPUs.
773774 Note: The authors of Eurus-PRIME only published results from training on Qwen2.5-Math-7B.
775 Therefore, we do not include results for the Qwen2.5-7B model in our comparison.
776777 **C SUPPLEMENTARY EXPERIMENT**
778779 **C.1 EFFECT OF METRIC SELECTION**780 Table 7: Ablation study comparing our proposed node-level modification metric (‘Fix’) with a
781 branch-level ‘Pruning’ metric. ‘Fix’ consistently outperforms ‘Pruning’, validating our fine-grained
782 approach.
783

784 Model	AIME24	AIME25	AMC23	MATH500	Minerva	Olympiad	Avg.
785 Fix							
786 Re-Schedule _{linear}	34.2	15.6	72.4	81.2	36.4	42.5	47.1
787 Re-Schedule _{sigmoid}	34.2	16.0	71.1	81.8	42.3	44.4	48.3
788 Pruning							
789 Re-Schedule _{linear}	35.7	14.6	73.7	81.0	34.9	41.6	46.9
790 Re-Schedule _{sigmoid}	33.1	16.7	71.1	82.0	39.0	42.4	47.4

793 We validate our core design choice for the r-score calculation. Our proposed method (‘Fix’) defines
794 an ‘edit’ as a single node modification. We compare this against an alternative (‘Pruning’), where an
795 ‘edit’ is defined as pruning an entire sub-branch from a decision point. Table 7 shows that the ‘Fix’
796 method consistently outperforms ‘Pruning’ for both linear (47.1% vs. 46.9%) and sigmoid (48.3%
797 vs. 47.4%) schedules. This result shows that compared with the branch ‘Pruning’, the node ‘Fix’ is
798 more consistent with the training process of reinforcement learning.
799800 **C.2 VARIANCE ANALYSIS**
801802 Table 8: Variance of Re-Schedule over multiple runs.
803

804	AIME24	AIME25	AMC23	MATH500	Minerva	Olympiad
805 Avg. \pm Var.	35.2 ± 0.1	16.0 ± 0.0	72.3 ± 0.4	82.2 ± 0.0	42.3 ± 0.6	44.4 ± 0.6

806 To assess the stability of our proposed Re-Schedule method, we conducted repeated experiments
807 using different random seeds. Table 8 reports the variance. The results demonstrate that our method
808 exhibits low variance. This confirms that the reported improvements are statistically stable and
809

810 not due to random variation. Compared to performance improvements, the impact of variance is
 811 minimal.

813 C.3 ABLATION ON TOKEN INTERVAL l

815 To investigate the impact of l on performance and its relationship with model capabilities, we con-
 816 ducted ablation studies on two base models: Qwen2.5-Math-7B and Qwen2.5-7B. We utilized the
 817 Sigmoid weighting mapping for these experiments.

818 Table 9 summarizes the average accuracy across six benchmarks (AIME24, AIME25, AMC23,
 819 MATH500, Minerva, Olympiad) for varying token intervals $l \in \{200, 400, 600, 1200\}$.

821 Table 9: Impact of Token Interval l on Average Accuracy (Sigmoid Mapping).

823 Interval (l)	824 Qwen2.5-Math-7B (Avg)	824 Qwen2.5-7B (Avg)
825 $l = 200$	826 48.3	826 44.5
826 $l = 400$	827 48.6	827 43.2
827 $l = 600$	828 48.9	828 43.1
828 $l = 1200$		41.1

829 The results indicate that Re-Schedule is generally robust to the choice of l within the range of
 830 [200, 600]. For the specialized math model (Qwen2.5-Math-7B), performance remains high and
 831 stable as l increases to 600. For the general model (Qwen2.5-7B), while $l = 200$ yields the best
 832 results, the performance drop at $l = 600$ is relatively contained. A significant performance drop
 833 is observed for both models when $l = 1200$. This suggests that when the interval is too large, the
 834 approximated reasoning tree becomes too coarse to capture the critical branching points necessary
 835 for effective r-score estimation.

837 C.4 SENSITIVITY TO BRANCHING FACTOR k , DEPTH d AND MODIFICATION BUDGET M

839 We investigated the impact of the reasoning tree size on performance by varying the branching factor
 840 k and depth d on the Qwen2.5-Math-7B model.

842 Table 10: Ablation study on branching factor k (with fixed $d = 4$).

844 Setting	845 AIME24	845 AIME25	845 AMC23	845 MATH500	845 Minerva	845 Olympiad	845 Avg
<i>Linear Mapping</i>							
$k = 3$	32.5	15.2	74.0	81.8	36.3	41.0	46.8
$k = 4$ (Default)	34.2	15.6	72.4	81.2	36.4	42.5	47.1
$k = 5$	35.1	18.1	77.4	81.8	37.8	44.6	49.1
<i>Sigmoid Mapping</i>							
$k = 3$	32.0	15.2	74.2	81.6	38.6	43.1	47.5
$k = 4$ (Default)	34.2	16.0	71.1	81.8	42.3	44.4	48.3
$k = 5$	36.4	17.0	75.5	81.2	40.6	43.4	49.0

854 **Varying branching factor k :** Fixing $d = 4$ and $l = 200$, we tested $k \in \{3, 4, 5\}$. As shown in
 855 Table 10, increasing k generally improves performance, suggesting that a denser tree captures the
 856 structural difficulty more accurately.

857 **Varying tree depth d :** Fixing $k = 4$ and $l = 200$, we tested $d \in \{2, 3, 4\}$. Table 11 shows that
 858 deeper trees provide a better estimation of the reasoning structure, leading to improved downstream
 859 performance.

861 **Varying node modification budget M :** Finally, we assess the stability of our method with respect
 862 to the node modification budget M . Fixing $k = 4, d = 4$, and $l = 200$, we evaluated performance
 863 across $M \in \{5, 10, 15\}$. As presented in Table 12, the results are relatively robust to changes in
 this parameter. While the default setting of $M = 10$ yields the optimal average accuracy, varying

864
865Table 11: Ablation study on tree depth d (with fixed $k = 4$).

Setting	AIME24	AIME25	AMC23	MATH500	Minerva	Olympiad	Avg
<i>Linear Mapping</i>							
$d = 2$	31.1	15.3	74.2	81.8	38.2	42.2	47.1
$d = 3$	31.4	14.6	72.7	82.0	39.7	43.3	47.3
$d = 4$ (Default)	34.2	15.6	72.4	81.2	36.4	42.5	47.1
<i>Sigmoid Mapping</i>							
$d = 2$	31.9	14.8	74.5	81.6	37.2	42.4	47.1
$d = 3$	33.2	16.4	73.0	80.0	41.9	41.6	47.7
$d = 4$ (Default)	34.2	16.0	71.1	81.8	42.3	44.4	48.3

866
867
868
869
870
871
872
873
874
875
876
877
878
879
880
881
882
883
884
885
886
887
888
889
890
891
892
893
894
895
896
897
898
899
900
901
902
903
904
905
906
907
908
909
910
911
912
913
914
915
916
917Table 12: Ablation study on node modification budget M (with fixed $k = 4, d = 4, l = 200$).

Setting	AIME24	AIME25	AMC23	MATH500	Minerva	Olympiad	Avg
$M = 5$	33.6	15.4	72.2	79.0	40.4	43.1	47.3
$M = 10$ (Default)	34.2	16.0	71.1	81.8	42.3	44.4	48.3
$M = 15$	34.7	16.0	71.8	82.0	41.6	42.4	48.1

the budget between 5 and 15 results in no significant performance degradation, indicating that the r-score remains a reliable metric across different budget constraints.

C.5 GENERALIZATION TO DIFFERENT MODEL ARCHITECTURES

To demonstrate the broad applicability of our method beyond the Qwen2.5 family, we conducted additional experiments on the Qwen3-4B-Base model.

Table 13: Performance comparison on Qwen3-4B-Base.

Model	AIME24	AIME25	AMC23	MATH500	Minerva	Olympiad	Avg
GRPO	24.2	21.8	52.4	86.0	39.4	43.4	44.5
ACC	24.8	23.3	59.3	88.8	41.6	42.0	46.6
Re-Schedule (Ours)	27.6	26.9	57.6	89.8	43.5	47.4	48.8

As shown in Table 13, Re-Schedule consistently outperforms both the standard GRPO baseline and the accuracy-based curriculum (ACC) across all benchmarks. This confirms that the effectiveness of the r-score is not limited to specific model architectures or sizes.

918 C.6 DYNAMIC R-SCORE CALCULATION
919920 To determine if the r-score should be updated as the model evolves, we compared our standard
921 static approach (computed once before training) with a dynamic approach where the r-score is re-
922 computed and weights are updated three times during the training process.923 Table 14: Comparison between Static and Dynamic R-Score updates on Qwen2.5-Math-7B.
924

926 Method	927 AIME24	928 AIME25	929 AMC23	930 MATH500	931 Minerva	932 Olympiad	933 Avg
<i>Linear Mapping</i>							
928 Static (Default)	929 34.2	15.6	72.4	81.2	36.4	42.5	47.1
928 Dynamic (3 updates)	929 34.6	14.9	75.3	80.0	39.7	41.6	47.8
<i>Sigmoid Mapping</i>							
931 Static (Default)	932 34.2	16.0	71.1	81.8	42.3	44.4	48.3
931 Dynamic (3 updates)	932 35.3	15.2	74.2	82.4	42.7	43.6	48.9

934 As shown in Table 14, the dynamic approach yields performance comparable to the static baseline
935 (e.g., 48.9% vs. 48.3% for Sigmoid mapping). Given the substantial computational cost of re-
936 generating reasoning trees during training, we conclude that the static r-score serves as a sufficient
937 and efficient prior for guiding the curriculum.938 C.7 GENERALIZATION TO CODE GENERATION
939940 Table 15: Performance comparison on Code Generation (LiveCodeBench v5).
941

942 Method	943 pass@1	944 pass@4
944 GRPO	25.4	35.4
945 ACC _{sigmoid}	25.8	36.0
946 Re-Schedule _{sigmoid}	26.3	37.8

947 To validate the generalization capability of Re-Schedule beyond mathematical reasoning, we ex-
948 tended our evaluation to the domain of Code Generation. We utilized DeepSeek-R1-Distill-Qwen-
949 1.5B as the base model. The model was trained on the ArcherCodeR dataset Wang et al. (2025a),
950 which contains 6,753 code generation tasks. For evaluation, we used the LiveCodeBench v5 bench-
951 mark Jain et al. (2024). We report pass@1 and pass@4 metrics (averaged over 8 samples).952 As shown in Table 15, Re-Schedule consistently outperforms both the standard GRPO baseline and
953 the accuracy-based curriculum (ACC). Specifically, our method achieves a +0.9% improvement in
954 pass@1 and a significant +2.4% improvement in pass@4 compared to GRPO. These results confirm
955 that the structural insights captured by the r-score are effective in the coding domain, where the
956 “reasoning tree” corresponds to the decision space of code logic and syntax.